Operational Characteristics of Non-firm Wind Generation in Distribution Networks

M. Džamarija, *Student Member, IEEE,* M. Bakhtvar and A. Keane, *Member, IEEE*

***Abstract*—Distributed wind generation is growing on power systems across the world. It presents many well established technical issues in the distribution network, such as voltage rise, network reinforcement requirements or varying power output. Non-firm generation, i.e. one to which curtailment can apply due to network infrastructure technical constraints, potentially holds certain benefits for distributed wind generation. This paper will demonstrate the operational characteristics of non-firm wind generation, without the need for network reinforcements. It also proposes an AC optimal power flow model used for evaluating the maximum capacity of wind generation and time series AC optimal power flow for time series calculation in order to determine the energy output that this type of allocation will make during the operation stage. Results show that a significant increase of energy output from non-firm wind generation connected to distribution networks can be achieved in comparison to the commonly used firm type of allocation.**

***Index Terms*—distribution networks, optimal power flow, wind generation**

I. Nomenclature

(TS) AC OPF sets, parameters and variables are defined.

Sets

GC	Set of generation capacity (indexed by gc)
W	Set of wind farms (indexed by w)
SG	Set of slack generators (indexed by sg)
B	Set of buses (indexed by b)
L	Set of lines and transformers (indexed by l)
T	Set of time steps (indexed by t)

Variables

$(V,\delta)_b$	Voltage magnitude and voltage angle at b
$(p,q)_w$	(P,Q) output of w
$(p,q)_{gc}$	(P,Q) output of gc
$(p,q)_{sg}$	(P,Q) output of sg
$(p,q)_l^{(n,m)}$	(P,Q) injection onto l at (start, end) bus
$i_l^{(n,m)}$	Current injection onto l at (start, end) bus

Parameters

$(r,x)_l$	Resistance and reactance of l
$(p,q)_b^{(-,+)}$	(min/max) (P,Q) demand at b
$(p,q)_b$	(P,Q) demand at b
$V_b^{(-,+)}$	(min/max) voltage magnitude at b
V_{ref}	Voltage magnitude at b_r
b_r	Reference bus
$(p,q)_w^{(-,+)}$	Available active and reactive power for w
p_{gc}^{+}	Allocated generation capacity for gc
β_{gc}	Location of gc
β_w	Location of w
β_{sg}	Location of sg
$\beta_l^{(n,m)}$	(start,end) bus of l
i_l^{MAX}	Maximum current magnitude of element l (kA)
t	Time step

II. Introduction

WIND generation allocation is increasing in distribution networks. Given that these resources are generally sited in remote areas, they present well established issues in distribution networks, such as network reinforcement requirements and voltage rise. Firm connection of wind generation implies large investments in new distribution network assets. This paper proposes an alternative operation approach that might delay investments in the network infrastructure.

Firm generation allocation is a traditional and prevailing approach to power system planning. Firm generation capacity allocation entails that a generator is allowed to output full power at any given time, irrespective of other variables in the network, such as demand, dynamic line ratings or network configuration [1]. This can result in suboptimal use of distribution network capacity. The assessment of firm allocation typically focuses on maximum generation at minimum demand, usually the worst-case condition for distribution networks. Maximum wind generation power output occurs rather infrequently and coincides with minimum demand rarely. An alternative type of connection policy is referred to as non-firm, i.e. one to which curtailment can apply due to network infrastructure technical constraints [2]. Although, at some stages, there is the need for wind power curtailment, non-firm connection would allow most of the wind energy potential to be exploited, without network reinforcements. Nevertheless, it remains important to estimate, in a preliminary feasibility study, how

This work was conducted in the Electricity Research Centre, University College Dublin, Ireland, which is supported by the Commission for Energy Regulation, Bord Gáis Energy, Bord na Móna Energy, Cylon Controls, EirGrid, EPRI, ESB International, ESB Power Generation, ESB Networks, Gaelectric, Intel, SSE Renewables, SWS Energy, UTRC and Viridian Power & Energy. M. Džamarija and A. Keane are supported by Science Foundation Ireland under Grant Number 06/CP/E005. The authors are with University College Dublin (e-mail: mario.dzamarija@ucdconnect.ie).

much energy curtailment may occur in order to find out if the investment in wind farms (WF) is economically viable.

Non-firm generation capacity allocation is addressed in the following works: [1], [3]-[5]. In [1] and [4] generation capacity is considered to be an inter-period variable, while other variables are multi-period (change in between periods depending on the generation/demand). In [1], besides the initial set of generation capacity, a second set of generators, which are connected to the same buses, introduces curtailment. Curtailed energy is restricted by a defined curtailment factor. It is examined how the different values of curtailment factor affect the allocated non-firm capacity. In [3] a methodology is given that maximizes the energy from DG per euro of connection cost, while also minimizing the voltage rise. Minimization of the voltage rise consequently leads to minimization of curtailment or maximization of non-firm energy. In [5] several profiles of renewable sources (wind, wave and tidal), together with demand, are considered in an OPF model. Time series OPF calculations are used and OPF is deployed to allow extraction of the maximum amount of energy from available resources while maintaining operational limits of the network. It also examines the economic loss due to curtailment that a renewable generator may experience.

While the work described in [1], [3] and [4] primarily deals with the planning aspects of non-firm distributed generation, the focus of this paper is on the operational issues of non-firm distributed wind generation. In contrast to previously listed works, the planning method proposed in this paper will consider an artificial increase in network capacity for a non-firm generation allocation case, by raising thermal and voltage limits. As a part of this work two AC optimal power flow (AC OPF) models are introduced. These two models, which are used for planning and operation purposes, consider current as the thermal limit for each network element. The time series AC OPF (TS AC OPF) model is utilized for the operation stage in a similar way as it is presented in [5]. The TS AC OPF model has an asymmetrical capability diagram implemented as one of its functionalities. The capability diagram limits, defined by the model, can be arbitrarily modified in order to match any symmetrical or asymmetrical piecewise linear wind turbine capability diagram. This allows partial decoupling of the active and reactive power dispatch in the optimization process, whilst if using fixed power factor control, active and reactive power dispatch is bound together. Using TS AC OPF, the effects of network constraints on the active and reactive power dispatch of non-firm wind generation are examined.

The planning and operation optimization models are presented in Section III, followed by the case study description in Section IV. In Section V the results for firm and non-firm cases, for the planning and operation stages, are compared. Operational characteristics of non-firm wind generation are also discussed. A potential further research area and conclusion are given in Section VI.

III. Optimization Model

AC OPF is an industry accepted method for solving a wide range of both technical and economic power system optimization problems [6]-[8]. In order to find an optimal planning/operating point (minimum or a maximum of a certain variable) for a distribution network one needs to formulate a mathematical optimization problem that defines the power system and includes its technical data. If an AC power system is modeled, that calls for a non-linear programming approach, since the equality and inequality constraints in the models are non-linear. For the purposes of this case study an AC OPF model for the planning stage and a TS AC OPF model for the operation stage are utilized.

A. AC OPF Model (Planning Stage)

In the planning stage the AC OPF model is employed in order to assess available headroom for generation capacity using a single generation/demand scenario. Considering the issue of voltage rise, which is usually the most challenging problem when allocating distributed generation, the worst case of maximum generation at minimum load is studied. The allocation of generation capacity *gc* is maximized in the planning stage:

$$max \sum_{gc \in GC} p_{gc} . \tag{1}$$

The capability diagram considered in the AC OPF model is defined by reactive power limits at maximum active power output of a generator capacity according to (15).

B. TS AC OPF Model (Operation Stage)

The operation stage differs from the planning stage since it includes time variant generation and demand. The AC OPF model is run consecutively at each time step *t* in order to consider time changing wind and load. This model is referred to as TS AC OPF. Due to the time variant wind power, generation capacity *gc*, used in the AC OPF model, is replaced with WF *w*. Nominal power of WFs *w* matches allocated generation capacity p_{gc}^{+}, which has been determined previously in the planning stage. Available wind power p_{w}^{+}, as well as the demand $(p,q)_b$, is updated at each time step *t*, according to time series data:

$$p_w^+ = \omega_t \cdot p_{gc}^+ , \ \forall w \in W, \ \forall t \in T \tag{2}$$

$$(p,q)_b = \eta_t \cdot (p,q)_b^+ , \ \forall b \in B, \ \forall t \in T . \tag{3}$$

At time step *t*, η_t is the demand level relative to the peak and ω_t is the wind generation level relative to the allocated generation capacity p_{gc}^{+} determined in the planning stage. Parameter *t* is used as a time series iterations index.

The objective of the operation stage is to maximize energy export from the WFs to the grid supply point (GSP). If there is no wind curtailment required, then loss minimization is a sensible objective function. Otherwise, if curtailment is required, then maximization of WFs power output is a better choice for the objective function. Depending on the situation for each time step *t*, the appropriate objective function is applied. These two approaches are described as follows.

1) Loss minimization objective

For the time steps *t* in the operation stage, during which wind power is low, the objective function of the TS AC OPF model is loss minimization:

$$min \sum_{l \in L} \left(p_l^n + p_l^m \right). \quad (4)$$

Loss minimization, which is achieved by optimally dispatching reactive power of individual WFs according to (16), will consequentially lead to maximum energy export from WFs to the GSP. Active power dispatch of individual WFs is a predetermined variable, whereby it corresponds to wind power time series data (16).

2) Power output maximization objective

For the time steps *t*, that are found to be infeasible when conducting loss minimization (4), WF power curtailment is required, in order to solve the optimization model. For these individual time steps *t* the objective function of the TS AC OPF model is WFs power output maximization:

$$max \sum_{w \in W} p_w . \quad (5)$$

This is achieved by optimally dispatching active and reactive power of individual WFs. Active power is dispatched in the range of 70% to 100% of available wind power p_w^+ (17). That way up to 30% of the available wind power p_w^+ can be curtailed at every WF. The optimization process will allocate curtailment in a way such that only WFs violating the network constraints are curtailed, resulting in minimum overall curtailment, i.e. maximum total power output of all the WFs. The reactive power output of WFs is within capability diagram limits defined by (17) and is dispatched such that minimum curtailment can be achieved.

C. Equality Constraints

The active and reactive power flow injection onto the start bus *n* and the end bus *m* of element *l* is calculated according to Kirchhoff's Voltage Law (KVL):

$$p_l^{(n,m)} = p_{l,KVL}^{(n,m)} \left(\mathbf{V}, \boldsymbol{\delta} \right), \quad \forall l \in L \quad (6)$$

$$q_l^{(n,m)} = q_{l,KVL}^{(n,m)} \left(\mathbf{V}, \boldsymbol{\delta} \right), \quad \forall l \in L . \quad (7)$$

Kirchhoff's Current Law (KCL) – conservation of real and reactive power at bus *b*, used in the AC OPF model is defined:

$$\sum_{gc \in GC | b = \beta_{gc}} p_{gc} + \sum_{sg \in SG | b = \beta_{sg}} p_{sg} = \sum_{l \in L | b = \beta_l^{n,m}} p_l^b + p_b^- , \quad \forall b \in B \quad (8)$$

$$\sum_{gc \in GC | b = \beta_{gc}} q_{gc} + \sum_{sg \in SG | b = \beta_{sg}} q_{sg} = \sum_{l \in L | b = \beta_l^{n,m}} q_l^b + q_b^- , \quad \forall b \in B. \quad (9)$$

KCL used in the TS AC OPF model is defined:

$$\sum_{w \in W | b = \beta_w} p_w + \sum_{sg \in SG | b = \beta_{sg}} p_{sg} = \sum_{l \in L | b = \beta_l^{n,m}} p_l^b + p_b , \quad \forall b \in B \quad (10)$$

$$\sum_{w \in W | b = \beta_w} q_w + \sum_{sg \in SG | b = \beta_{sg}} q_{sg} = \sum_{l \in L | b = \beta_l^{n,m}} q_l^b + q_b , \quad \forall b \in B. \quad (11)$$

The lower voltage side of the distribution transformer is taken as the reference bus b_r with the voltage magnitude $V_{b_r} = V_{ref}$ and voltage angle $\delta_{b_r} = 0$.

D. Inequality Constraints

Current flowing at the start and the end of the line or a transformer *l* is restricted by the thermal constraint:

$$i_l^{(n,m)} \le i_l^{MAX} , \quad \forall l \in L. \quad (12)$$

Voltage magnitude at bus *b* is constrained by min/max value $V_b^{(-,+)}$:

$$V_b^- \le V_b \le V_b^+ , \quad \forall b \in B. \quad (13)$$

Voltage angle at bus *b* is constrained by min/max value:

$$-\pi \le \delta_b \le \pi , \quad \forall b \in B. \quad (14)$$

The capability diagram for allocated generation capacity *gc*, used in the AC OPF model, considers asymmetrical reactive power limits:

$$\left. \begin{aligned} & p_{gc} \ge 0 \\ & q_{gc} \ge - p_{gc} \cdot tan\left(arccos\, 0.96 \right) \\ & q_{gc} \le p_{gc} \cdot tan\left(arccos\, 0.98 \right) \end{aligned} \right\} \quad \forall gc \in GC . \quad (15)$$

Symmetrical and asymmetrical capability diagram limits for a WF *w*, used in the TS AC OPF model when minimizing losses:

$$\left. \begin{aligned} & p_w = p_w^+ \\ & q_w^- \le q_w \le q_w^+ \end{aligned} \right\} \quad \forall w \in W , \quad (16)$$

or when conducting curtailment:

$$\left. \begin{aligned} & 0.7 \cdot p_w^+ \le p_w \le p_w^+ \\ & q_w^- \le q_w \le q_w^+ \end{aligned} \right\} \quad \forall w \in W . \quad (17)$$

The minimum and maximum reactive power limit is defined for each wind farm *w* by a variable $q_w^{(-,+)}$ which depends on the active power dispatch p_w, the available wind power p_w^+ and the allocated generator capacity p_{gc}^+. These reactive power limits are defined in Appendix B as inequality constraints, and are calculated for each time step *t*. These limits can also be arbitrarily modified in order to match any piecewise linear wind turbine capability diagram. There are no limitations imposed on the slack generator, connected to the GSP, since it presents a strong transmission network.

E. Implementation and Model Validation

The (TS) AC OPF model presented is written in AIMMS optimization modeling environment [9]. Optimization problems in this paper are solved using both versions of the CONOPT NLP solver: 3.14G and 3.14V. CONOPT solver has

been developed by ARKI Consulting and Development, Denmark. In addition to OPF, AIMMS can also be used to solve power flow equations with a constant objective function. The NLP solver then looks for the only feasible solution (basic power flow problem) and acts as a nonlinear equation solver [10]. The AC OPF model is validated by comparing its results with results of power system analysis software: DIgSILENT PowerFactory [11]. The AC power flow results were found to be identical for a range of test calculations.

IV. Case Study

The (TS) AC OPF model is demonstrated on a representative Irish 6 bus 38 kV distribution network shown in Fig. 1. Minimum and maximum allowable voltage magnitude $V_b^{(-,+)}$ at bus b is set to 36.5 kV and 42.5 kV respectively since it is a common practice in Ireland to operate the 38 kV network within this voltage range. The set point for sending bus voltage (which is also the reference bus b_r in the two optimization models) is 41.6 kV and this set point applies on all rural/overhead line (OHL) networks. Thermal limits for the OHLs and the distribution transformer are set to nominal values and are as stated in Appendix C. Since the distribution network, used for the case study, consists of OHLs that have negligible shunt susceptance, these values are left out of (6) and (7). The case study consists of planning and operation stages.

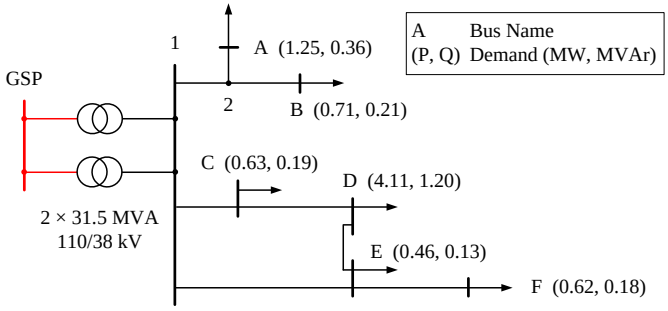

Fig. 1 Representative Irish distribution network at minimum demand

A. Planning Stage

The planning stage is divided into two separate cases: firm and non-firm generation capacity allocation.

1) Firm generation capacity allocation

Firm capacity allocation considers thermal and voltage limits in the network. It also considers an outage of one of the distribution transformers, in keeping with the N-1 criterion which is a standard practice in the distribution system planning.

2) Non-firm generation capacity allocation

The non-firm capacity allocation approach in this case study considers thermal and upper voltage limits 10% higher than the maximum allowed during normal operation as a means of facilitating extra generation capacity. This would imply that voltage magnitude V_b^+ at bus b is 46.75 kV. Thermal limits for OHLs are set 10% higher than the value considered in the case for firm capacity allocation.

B. Operation Stage

Following on from the planning stage, historical wind and demand time series data is used to capture the operational characteristic of the allocated generation capacity, as shown in Fig. 2. Wind time-series data are values recorded in May 2010 for an existing WF on the west coast of Ireland and are scaled according to the WFs installed power. The operation stage is run for every quarter hour period in May 2010, which totals 2976 time steps t.

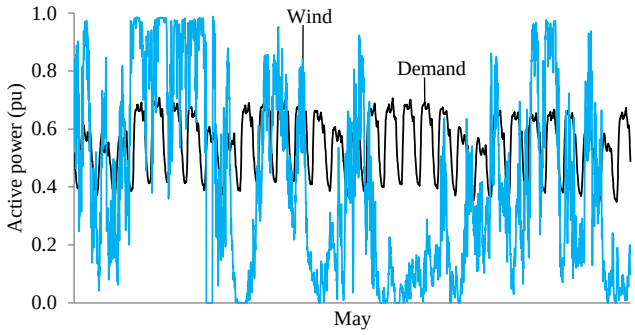

Fig. 2 Quarter hour wind power and demand, relative to peak values, 2010

The operation stage is divided into three separate cases.

1) Loss minimization

Minimization of losses (4) is the approach taken to find the results in this case. The nominal power of each WF w equals their respective generation capacity gc that is calculated in the firm allocation planning stage case. The capability diagram applied for WFs is shown in Fig. 3b. The depicted asymmetrical capability diagram applies to Vestas V90 3.0 MW wind turbine generators. It is noticeable that the capability diagram, for higher active power output, can consume more reactive power than it can produce.

2) Wind power curtailment without thermal constraints

The losses are minimized (4) for the time steps t that do not require power curtailment and the output power is maximized (5) for the time steps t that require power curtailment, i.e. no feasible solution found for loss minimization. The nominal power of each WF w equals their respective generation capacity gc that is calculated in the non-firm allocation planning stage case.

In this case the following simplifications are done: 1-thermal constraints are removed from the model, 2-capability diagram used for the WFs is a symmetrical one (Fig. 3a). Thermal limits are neglected in order to examine the effect of voltage constraints in isolation. The symmetrical capability diagram is used so that active and reactive power dispatch is decoupled, for higher wind power values. In cases where active power output value is higher than 22% of the rated WF power, reactive power can take any value between -0.505 pu and 0.505 pu (Fig. 3a).

This case is included in the case study in order to explain how the AC OPF model controls active and reactive power when operating non-firm wind generation.

3) Wind power curtailment with all constraints

This case is very similar to the previous one. The only differences are the inclusion of thermal constraints in the TS AC OPF model and replacing the symmetrical capability diagram with the asymmetrical one (Fig. 3b) for the existing WFs. Thermal limits are included in the optimization model in order to examine the effect of simultaneous binding thermal and voltage constraints on WFs active and reactive power dispatch.

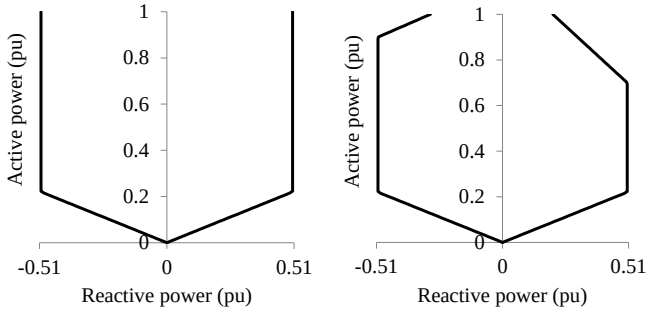

Fig. 3a Symmetrical PQ diagram b Asymmetrical PQ diagram

V. Results and Discussion

A. Planning Stage

The results for both the firm and non-firm planning cases are presented in Table I. The relaxation of voltage and thermal constraints, as well as ignoring the N-1 criterion, leads to a 64.33% increase in the allocated generation capacity *gc*: 42.63 MW for firm and 70.05 MW for non-firm capacity allocation. The locations of the generation capacity *gc*, as well as the binding thermal and voltage constraints in the test network, are shown in Fig. 4 and 5.

TABLE I COMPARISON OF FIRM AND NON-FIRM GENERATION CAPACITY ALLOCATION

Wind farm	Type of allocation	
	Firm (MW)	Non - firm (MW)
WF A	4.73	23.04
WF B	8.16	
WF C	13.70	12.84
WF D	7.87	
WF E	8.17	20.01
WF F		14.15
Total Capacity	42.63	70.05

1) Firm generation capacity allocation

For the firm planning case, voltage limits are dominant in constraining the generation capacity *gc* (one thermal and five voltage constraints in the network are binding), as shown in Fig. 4. The thermal limit of the transformer is constraining since the second transformer is switched off.

2) Non-firm generation capacity allocation

The voltage magnitude limit is not a dominant constraint for the generation capacity *gc* any more, since it is set to 46.75 kV, only as a means of facilitating extra generation capacity. Instead, the thermal constraints of OHLs are limiting the generation capacity allocation. One voltage and four thermal constraints in the network are binding, as shown in Fig. 5. The thermal constraint of the distribution transformers is not binding since both transformers are operating. The transformer outage is not considered in the non-firm allocation. In case one of them trips out, the WFs power will be curtailed.

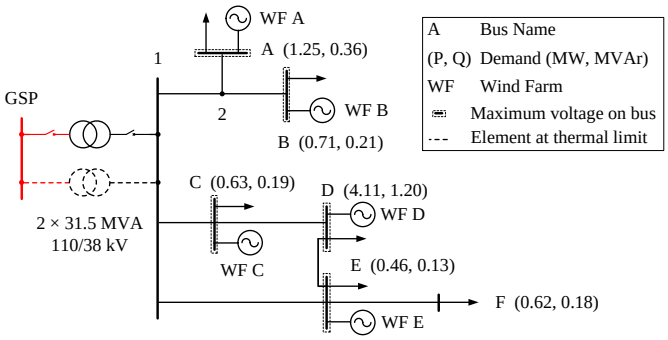

Fig. 4 Binding constraints in the test network and optimal allocation of firm generation capacity

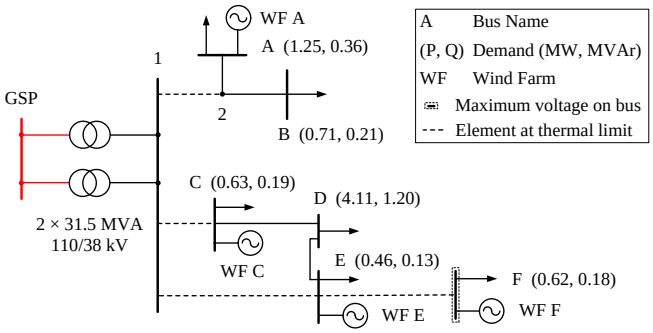

Fig. 5 Binding constraints in the test network and optimal allocation of non-firm generation capacity

B. Operation Stage

Results for all three operation stage cases are given in Table II. A significant increase in energy output from WFs is achieved, 58.93% if comparing the first case (12.84 GWh) and the third case (20.41 GWh). The percentage of energy increase would be the same as the percentage of generation allocation increase in the planning stage if there was no energy curtailment. Curtailed energy in the second and third case is 22 MWh and 693 MWh respectively. The number of time steps *t* during which curtailment is conducted is 102 for the second and 551 for the third operation stage case. The frequency of curtailment is increased in the third case since both thermal and voltage constraints in the distribution network are binding.

TABLE II COMPARISON OF THE THREE CASES IN THE OPERATING STAGE

Measurand	Case		
	First	Second	Third
WFs energy output (GWh)	12.84	21.08	20.41
Average Q import at GSP (MVAr)	1.12	11.58	9.72
Losses in test network (GWh)	0.18	1.34	1.11
Curtailed energy (%)	0	0.11	3.29
Number of curtailments	0	102	551

Average reactive power import from the transmission network, at GSP, in the first case is 1.12 MVAr. As the power output of WFs increases, an increase of reactive power consumption of the test network is noticeable,. As the wind power export increases, the distribution network has to import reac-

tive power in order to keep the operating voltage level within limits. For this reason average reactive power consumption in the second case is 11.58 MVAr, and in the third case 9.72 MVAr.

1) Wind power curtailment without thermal constraints

The AC OPF model, used in the non-firm planning stage, showes that bus F is the weakest in the 6 bus network with regard to the voltage rise, as shown in Fig. 5. In this case WF F, connected to bus F, is curtailed most frequently, for 102 out of 2976 time steps *t*, due to the voltage rise during windy periods. Fig. 6 demonstrates the calculated Q-V interrelation diagram, in respect of time, for the first week of May 2010. The first couple of days, when wind power is low, voltage magnitude values are below their allowed maximum (42.5 kV). During that time WF F is supplying demand with reactive power in order to minimize losses in the distribution network. The second half of the first week is characterized with higher wind power (as can be seen in Fig. 2). Consequently active power output increases and WF F has to consume reactive power in order to keep the voltage within the operating limits at bus F. Although reactive power capability of WF F is used to its limits (- 7.14 MVAr), for 102 time steps *t*, power curtailment will still be necessary in order to regulate the voltage rise (shaded parts in Fig. 6).

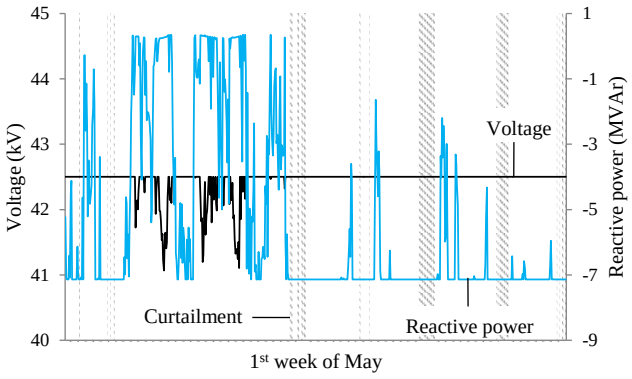

Fig. 6 Wind power curtailment without thermal constraints: Q-V interrelation diagram in respect of time for WF F connected to bus F, 2010

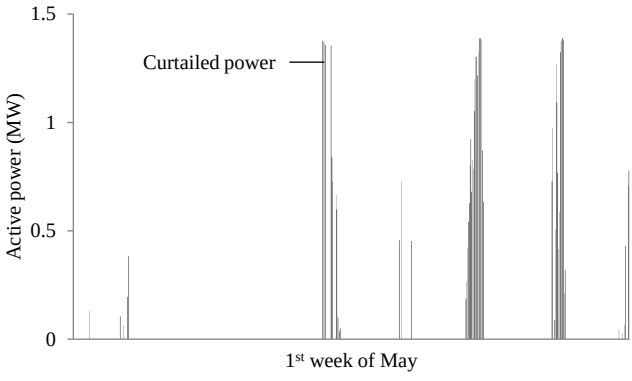

Fig. 7 Wind power curtailment without thermal constraints: WF F power curtailment diagram, 2010

The amount of curtailed power is displayed in Fig. 7 and shows that curtailment is only required during windy periods in the second half of the week, when WF F's power output is close to the nominal value. Power curtailment is also required for WFs A and E, because of the binding voltage constraint. For these WFs power curtailment is conducted for 15 out of 2976 time steps, since voltage rise at buses A and E is not as significant as it is for bus F.

2) Wind power curtailment with all constraints

In this operation stage case WF F, connected to bus F, is curtailed most frequently, for 551 out of 2976 time steps *t*. Fig. 8 demonstrates calculated Q-V interrelation diagram, in respect of time, for the first week of May 2010. Since both voltage and thermal constraints are binding, power curtailment of WF F is required although reactive power capability of the same WF has not been fully used. This is shown in shaded parts of Fig. 8, where dispatched Q is not represented by a straight line and it is not at its minimum value (- 7.14 MVAr), as it is in Fig. 6 for the previous case. The reason for this is the existance of two simultaneous binding constraints: voltage limit at bus F and current limit of OHL E – F. WFs increased absorbtion of the reactive power decreases the bus voltage magnitude but also increases the current flow in the line. For this reason power curtailment is necessary, in order to regulate the voltage rise, even though reactive power capability is not fully used. Thus reactive power cannot solve both binding constraints simultaneously and an increase in energy curtailment is required.

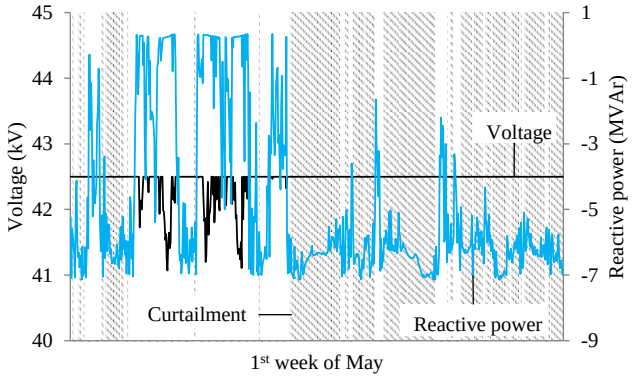

Fig. 8 Wind power curtailment with all constraints: Q-V interrelation diagram for WF F connected to bus F, 2010

It is important to mention that WFs active power dispatch p_w is below 81% of the nominal power p_{gc}^+ for the entire operation period in the third case. For this reason results depicted in the Fig. 8 will not be affected by the interdependency of p_w and q_w, as they only start to be coorelated for p_w equal or above 90% of p_{gc}^+ (Fig. 3b).

The amount and frequency of curtailed power output from WF F is increased because of the above mentioned reasons. Most of the curtailment will be required in the second half of the week during windy periods, as shown in Fig. 9.

WFs A and E also have to curtail power. WF A is curtailed for 527, and WF E for 40 out of 2976 time steps. It can be concluded that buses with more significant voltage rise require more curtailment from respective WFs.

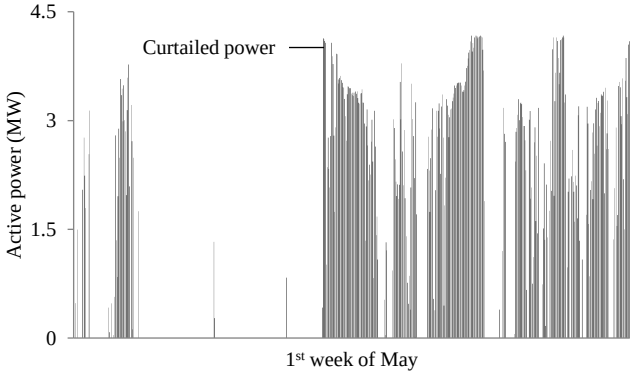

Fig. 9 Wind power curtailment with all constraints: WF F power curtailment diagram, 2010

The power curtailment in this case study is allocated in an optimal way, curtailing only the reqired active power of WFs that violate the constraints, resulting in minimum overall curtailment. In practice curtailment allocation usually depends on other non-technical aspects as well. For instance it can depend on an individual contract that the non-firm generator signs with the network operator. One of the types of contract is 'last-in, first-off', specifing the last connected generator as the first one to be curtailed. This can result in a sub-optimal operation of overall distributed generation assets and cause an increase of the curtailed energy. In future work, comparisons between existing curtailment strategies and the operational strategy presented in this paper could be made, showing the potential benefits of the latter.

VI. Conclusion

This paper introduces developed AC OPF and TS AC OPF models that are used for distribution planning and operation purposes respectively. It also proposes a method for non-firm generation allocation by an artificial increase in network capacity. AC OPF is applied on a test network in order to maximize allocation of firm and non-firm generation capacity. TS AC OPF is then used to extract maximum energy out of the allocated firm and non-firm generation, by minimizing losses or curtailed energy, in the observed time period. The results show a significant increase in capacity allocation and energy produced when comparing the firm and non-firm case.

As a part of the results operational characteristics of non-firm generation are shown and explained. It can be seen that in the case of binding voltage constraint, reactive power capability of WFs can be used to its limits, in order to minimize the curtailment. When both thermal and voltage constraints are binding, reactive power will not be able to deal with both constraints simultaneously and there will be an increase in energy curtailment. The interaction of simultaneous binding constraints and their effect on energy curtailment will be the focus of further work.

VII. Appendix

A. Supplement to Asymmetrical Capability Diagram

Reactive power limits are defined by inequality constraints (Fig. 3b), $\forall w \in W$:

$$0 \le p_w \le 0.22 \cdot p_{gc}^+$$
$$abs(q_w) \le p_w \cdot tan(arccos\,0.4) \quad (18)$$

$$0.22 \cdot p_{gc}^+ < p_w \le 0.9 \cdot p_{gc}^+$$
$$q_w \ge -0.22 \cdot p_{gc}^+ \cdot tan(arccos\,0.4) \quad (19)$$

$$0.9 \cdot p_{gc}^+ < p_w \le p_{gc}^+$$
$$q_w \ge -\left(\left(0.22 \cdot tan(arccos\,0.4)\right) - tan(arccos\,0.96)\right) \cdot \left(p_{gc}^+ - p_w\right) / 0.1 - p_{gc}^+ \cdot tan(arccos\,0.96) \quad (20)$$

$$0.22 \cdot p_{gc}^+ < p_w \le 0.7 \cdot p_{gc}^+$$
$$q_w \le 0.22 \cdot p_{gc}^+ \cdot tan(arccos\,0.4) \quad (21)$$

$$0.7 \cdot p_{gc}^+ < p_w \le p_{gc}^+$$
$$q_w \le \left(\left(0.22 \cdot tan(arccos\,0.4)\right) - tan(arccos\,0.98)\right) \cdot \left(p_{gc}^+ - p_w\right) / 0.3 + p_{gc}^+ \cdot tan(arccos\,0.98) \quad (22)$$

B. Security Constrained AC OPF

The security constraint can also be implemented in the AC OPF model to consider the loss of line, but it has not been used for planning purposes in this case study. The security constraint makes sure that the remaining network is operating within allowed limits. This constraint considers active power dispatch as an inter-period variable (i.e. p_w), while other variables change depending on the contingencies c ($V_{b,c}$, $q_{w,c}$, $p_{l,c}^{(n,m)}$etc.). It also means adding multiple network topologies to the model and increasing the size of the optimization problem.

C. Distribution Network Data

Table III Resistance, reactance and thermal limit of lines and transformers used in the test network

Start-end bus	r_l (Ω)	x_l (Ω)	i_l^{MAX} (kA)	Element
GSP – 1	0.24	5.57	0.48	Transformer
GSP – 1	0.24	5.57	0.48	Transformer
1 – 2	5.45	5.72	0.24	OHL
1 – C	2.45	2.62	0.24	OHL
2 – A	4.09	4.37	0.31	OHL
2 – B	1.39	1.48	0.30	OHL
C – D	5.64	6.01	0.24	OHL
D – E	2.96	3.14	0.24	OHL
E – 1	6.34	6.66	0.24	OHL
E – F	11.34	11.92	0.16	OHL

VIII. Acknowledgment

The authors thank ESB Networks for providing technical input data.

IX. References

[1] L. F. Ochoa, C. J. Dent, G. P. Harrison, 'Distribution Network Capacity Assessment: Variable DG and Active Networks,' *IEEE Tran. Power Systems*, vol. 25, pp. 87-95, Feb. 2010

[2] D. J. Burke, M. J. O'Malley, 'Factors Influencing Wind Energy Curtailment,' *IEEE Tran. Sustainable Energy*, vol.2, pp. 185-193, Apr. 2011

[3] A. Keane, M. O'Malley, 'Optimal Utilization of Distribution Networks for Energy Harvesting,' *IEEE Tran. Power Systems*, vol. 22, pp. 467-475, Feb. 2007

[4] L. F. Ochoa and G. P. Harrison, 'Using AC Optimal Power Flow for DG planning and optimisation,' *2010 IEEE Power and Energy Society General Meeting*, pp. 1-7

[5] T. Boehme, G.P. Harrison, A.R. Wallace, 'Assessment of distribution network limits for non-firm connection of renewable generation,' *IET Renewable Power Generation*, vol. 4, pp. 64-74, Jan. 2010

[6] H. W. Dommel, W. F. Tinney, 'Optimal Power Flow Solutions,' *IEEE Tran. Power Apparatus and Systems*, vol. PAS-87, pp. 1866 - 1876, Oct. 1968

[7] P. Siano, P. Chen, Z. Chen, A. Piccolo, 'Evaluating maximum wind energy exploitation in active distribution networks,' *IET Generation, Transmission & Distribution*, vol. 4, pp. 598-608, May 2010

[8] R. Zarate-Mihano, A. J. Conejo, F. Milano, 'OPF-based security redispatching including FACTS devices,' *IET Generation, Transmission & Distribution*, vol. 2, pp. 821-833, Nov. 2008

[9] M. Roelofs and J. Bisschop, *AIMMS—The User's Guide*. Haarlem, The Netherlands: Paragon Decision Technology, 2011.

[10] C. J. Dent, L. F. Ochoa, G. P. Harrison, J. W. Bialek, 'Efficient Secure AC OPF for Network Generation Capacity Assessment,' *IEEE Tran. Power Systems*, vol. 25, pp. 575-583, Feb. 2010

[11] DIgSILENT PowerFactory: *PowerFactory User's Manual V14.0*, Gomaringen, Germany: DIgSILENT GmbH, 2008.

X. Biographies

Mario Džamarija (S'2005) received the M.E.E. degree in 2007 from the Faculty of Electrical Engineering and Computing, University of Zagreb.

He is currently a postgraduate student at the School of Electrical, Electronic & Communications Engineering, University College Dublin with research interests in power system operation, distributed energy resources and optimal power flow.

Mostafa Bakhtvar received his B.Sc. degree in electric-power engineering from Islamic Azad University, Saveh Branch, Iran in 2010.

He is currently studying for his M.E. degree in energy systems engineering at University College Dublin, Ireland. His research interests include power system stability and optimal power flow

Andrew Keane (S'04-M'07) received B.E. and Ph.D. degrees in Electrical Engineering from University College Dublin in 2003 and 2007 respectively.

He is a lecturer with the School of Electrical, Electronic & Communications Engineering, University College Dublin with research interest in power systems planning and operation, distributed energy resources and distribution networks.